optica

Dynamic-disorder-induced enhancement of entanglement in photonic quantum walks: supplementary material

QIN-QIN WANG[1,2], XIAO-YE XU[1,2], WEI-WEI PAN[1,2], KAI SUN[1,2], JIN-SHI XU[1,2], GENG CHEN[1,2], YONG-JIAN HAN[1,2*], CHUAN-FENG LI[1,2†], AND GUANG-CAN GUO[1,2]

[1]CAS Key Laboratory of Quantum Information, University of Science and Technology of China, Hefei 230026, China
[2]Synergetic Innovation Center of Quantum Information and Quantum Physics,University of Science and Technology of China, Hefei 230026,China

[*]Corresponding author: smhan@ustc.edu.cn
[†]Corresponding author: cfli@ustc.edu.cn

Published 17 September 2018

This document provides supplementary information to "Dynamic-disorder-induced enhancement of entanglement in photonic quantum walks," https://doi.org/10.1364/optica.5.001136. We provide the detailed description of the experiment setup and the Lempel-Ziv complexity of sequences.

1. THE DETAILS OF THE EXPERIMENT SETUP

Experimental time multiplexing photonic DTQWs — In this work, the QWs is based on the time multiplexing protocol. However, for overcoming the problem of the extra loss, birefringence crystal are used to replace the asymmetric Mach-Zehnder interferometer and implement the spin-orbit coupling. Heralded single photons generated in SPDC are employed as the walker, the polarization is employed as the coin space, such that its polarization state can be rotated to any of the single qubit states by wave plates, and the arriving time of the photons, encoded in time bin, acts as the position space. One step quantum walk is realized by a module composed of a half-wave plate (HWP) or a quarter-wave plate (QWP) and one piece of birefringence crystal. The coin rotation operator implemented by the former is

$$\hat{R}_{\mathrm{HWP}}(\theta) = e^{-i2\theta\hat{\sigma}_y}\hat{\sigma}_z, \hat{R}_{\mathrm{QWP}}(\theta) = e^{-i\theta\hat{\sigma}_y}e^{-i(\pi/4)\hat{\sigma}_z}e^{i\theta\hat{\sigma}_y}. \quad (1)$$

where θ is the rotation angle of the optical axis of the wave plate, and $\hat{\sigma}_i$ denotes the Pauli matrices such that the eigenstates of the coin are $|H\rangle$ and $|V\rangle$, corresponding to the horizontal and vertical polarizations respectively, with the condition $\hat{\sigma}_z|H\rangle = |H\rangle$ and $\hat{\sigma}_z|V\rangle = -|V\rangle$. The birefringence of the latter causes the horizontal components to travel faster inside the crystal than the vertical one. Then, after passing through the crystal, the photons in the horizontal polarization move a step forward. Considering the dispersion after passing through a large number of crystals and the fact that the time bin encoding the position of the walker in reality is a single pulse with a typical duration of a few hundred femtoseconds, such a shift in time should be sufficiently large to distinguish the neighborhood pulses at last. The magnitude of the polarization-dependent time shift by the birefringence crystal depends on the crystal length and the cut angle. In this experiment, for introducing as weak dispersion as possible with sufficiently large birefringence, calcite crystal is adopted for its high birefringence index (0.167 at 800 nm), and the length is chosen to be 8.98 mm with the optical axis parallel to incident plane, such that the time shift is designed to be 5 ps for one-step quantum walk.

Heralded single photon adopted as the walker — The time multiplexing protocol requires pulse photons, which can be obtained by attenuating a pulse laser or modulating a continuous laser with an optical chopper. Considering the tradeoff between the operation on the time bins and the final analysis in the time domain, the time duration covers a range from tens to thousands picoseconds, reaching even a few microseconds. In our experi-

ment, for adopting a genuine single photon as the walker and considering that the length of the crystals for realizing the time shifter should be as short as possible to reduce dispersion and improve stability, the pulse duration of the single photon should be as small as possible; it is selected on the level of hundreds of femtoseconds here. Such a short single photon pulse can be generated from SPDC with an ultrashort femtosecond pulse laser as the pump. The generated photon pairs are time correlated, and as a result, the click of detection on the idler photon can predict the existence of the signal photon. Various architectures exist for generating this type of heralded single photons from SPDC. Here, considering the features of high brightness and collection efficiency, we adopt the beamlike SPDC. Then, the length of the nonlinear crystal can be chosen to be short.

Frequency up conversion single photon detection — The spectrum of the arriving time of single photons is usually obtained by the technology of time correlated single photon counting based on commercial single photon detectors. However, in our case, the signals are contained in a single photon pulse train with a pulse duration of approximately 1 ps and a repetition of 5 ps. Counting and analysis such ultra-fast single photon signals is challenging. The time resolution of commercial single photon detectors is limited by the time jitter, which is typically in the range of tens to hundreds picoseconds. As a result, it is unsuitable to directly use any commercial single photon detectors in this experiment. The detection of single photons with high resolution in time can be realized by transforming the temporal resolution to a spatial resolution. Based on the optical parameter up conversion, the measurement of an ultra-fast pulse of single photons can be realized by optical autocorrelation. That is, using an ultra-fast laser pulse to pump a nonlinear crystal, when the single photon and laser pulse meet each other inside the crystal, the single photon will be up-converted to have a short wavelength for the sum frequency process. For the photons with a long wavelength can be converted to a short one, this technology has been widely used in quantum communication for improving the detection efficiency in the infrared waveband. Here, we adopt this technology for its high resolution in time. Although periodically poled crystals are widely used in this technology for their high conversion efficiency, they are useless here for concentrating on the time resolution. The thickness of nonlinear crystal should be as thin as possible meanwhile taking into account the conversion efficiency. There exist two types of structures, collinear and non-collinear sum frequency. We adopt the latter to obtain a better signal to noise ratio (SNR), induced by the spatial divergence between the sum frequency signal and the pump laser. In this work, the crystal used is a 1 mm thick β-BaB_2O_4 (BBO) crystal, cut for type-II second harmonic generation in a beam like form. Then, the incidence angles of the signal pulse train with single photons and the pump laser are equal to each other, with 3° to the normal direction. For reducing the noise induced by the strong pump laser, a dispersion prism in a 4F system is adopted as a spectrum filter. The scattered photons with wavelength longer than 395 nm are blocked by a knife edge. The rising edge in the sideband of this self-established spectrum filter is less than 1 nm.

Description of the experimental setup — An ultra fast pulse (140 fs) train generated by a mode-locked Ti:sapphire laser with a central wavelength at 800 nm and repetition ratio 76 MHz is firstly focused by lens L1 to shine on a 2 mm thick β-BaB_2O_4 crystal (BBO1), cut for type-I second harmonic generation. The frequency-doubled ultraviolet pulse (with a wavelength centered at 400 nm, 100 mW average power and horizontally polarized) and the residual pump laser are collimated by lens L2, and then separated by a dichroic mirror (DM). The frequency-doubled pulse train is then focused by lens L3 to pump the second nonlinear crystal (BBO2), cut for type-II nondegenerate beam like SPDC. The signal and idler photons are collimated together with one lens L4 (f=150 mm). The collimated signal photons in horizontal polarization with a center wavelength at 780 nm are then guided directly in free space to the following quantum walks device. The collimated idler photons in vertical polarization with a center wavelength of approximately 821 nm firstly pass through a spectrum filter with a central wavelength 820 nm and bandwidth 12 nm and then are coupled into a single-mode fibre and sent directly to a single-photon avalanche diode (SPAD) for counting in coincidence with the signal photons. The quantum walks device is composed of HWPs (QWPs) and calcite crystals, and each step contains one piece of HWP (QWP) and one piece of calcite crystal. In the experiment, we have adopted

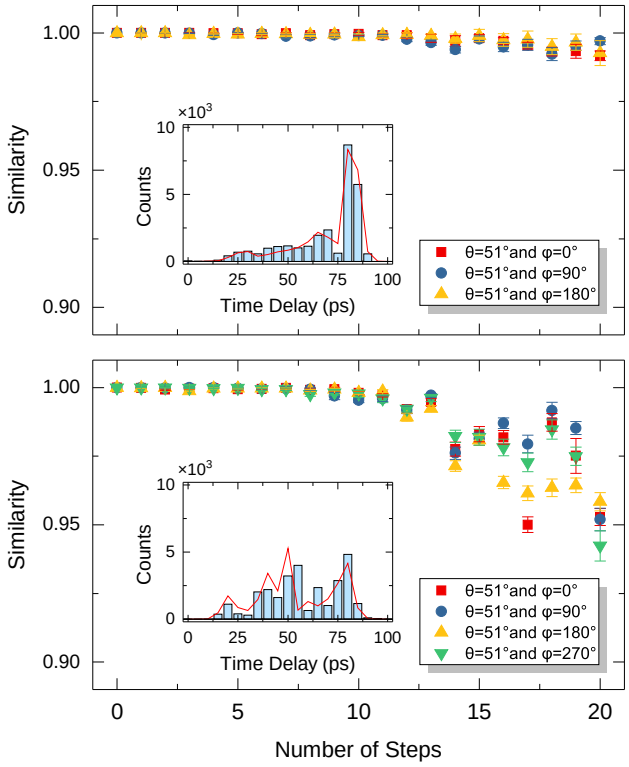

Fig. S1. Plot of the similarity for each step of QW. The similarity is defined as $S = \sum_x \sqrt{P_{\rm exp}(x)P_{\rm th}(x)}$, where $P_{\rm exp}$ stands for the experimental probability distribution and $P_{\rm th}$ is the corresponding theoretical prediction. The results for ordered QW are shown in the top panel and the results for dynamically disordered QW are presented in the bottom panel. The inset in each panel shows the coincidence counts after a 20-step walk for a initial state with $\theta = 51°$ and $\phi = 0°$. In the ordered scenarios, the similarity becomes degenerate gradually as the number of steps increases, mainly for the decoherence. In the disordered scenarios, there are more occupations near the origin (in the middle of time delays), where the interference is more complicated, results the faster degeneration of the similarity compared to the ordered cases. Only statistical errors are considered with total counts 24 thousand in 4 hundred seconds.

20 such sets, with only 1/4 of them shown in the figure. The initial state is prepared by an apparatus composed of a polarized beam splitter (PBS1), a half wave plate (HWP1) and a quartz wave plate (QWP1). The residual pump in the frequency-double process is adopted as the pump in the following frequency up conversion single photon detection with the retroreflector R1 for temporal matching. After the quantum walks is finished, the signal photons are collected into a short single mode fibre (10 cm long) by a fibre collimator (FC1) and then guided to the polarization analyzer composed of QWP2, HWP2 and PBS2 successively. Finally, the arriving time of signal photons is measured by scanning the pump laser and detecting the up conversion signals with a photomultiplier tubes (PMT). For reducing the scattering noise, BBO3 is cut for noncollinear up conversion and a spectrum filter based on a 4F system is constructed, where a prism is adopted for introducing the dispersion, a knife edge is used to block the long waves and the signal is reflected to the PMT with a pickup mirror.

2. LEMPEL-ZIV COMPLEXITY

Lempel-Ziv (LZ) complexity can be introduced to estimate the randomness of finite sequences, in the spirit of the Kolmogorov complexity. The LZ complexity measure counts the number of distinct substrings (patterns) in a sequence when scanned from left to right and then parsed. Note that we only consider binary sources throughout this paper. The algorithm is as follows [1]:

1. Let $S_C = s_1 s_2 \cdots s_n$ denote a finite 0-1 symbolic sequence; $S_C(i,j)$ denotes a substring of S_C that starts at position i and ends at position j, that is, when $i \leqslant j$, $S_C(i,j) = s_i s_{i+1} \cdots s_j$ and when $i \geqslant j$, $S_C(i,j) = \{\}$ (null set); $V(S_C)$ denotes the vocabulary of a sequence S_C. It is the set of all substrings $S_C(i,j)$ of S_C, (i.e., $S_C(i,j)$ for $i = 1, 2 \cdots n$; $i \leqslant j$). For example, let $S_C = 010$, we then have $V(S_C) = \{0, 1, 01, 10, 010\}$.

2. The parsing procedure needs to scan the sequence S_C from left to right. If $S_C(i,j)$ belongs to $V(S_C(1, j-1))$, then $S_C(i,j)$ and $V(S_C(1, j-1))$ is renewed to be $S_C(i, j+1)$ and $V(S_C(1,j))$, respectively. Repeat the previous process until the renewed $S_C(i,j)$ does not belong to the renewed $V(S_C(1, j-1))$, then place a dot after the renewed $S_C(i,j)$ to indicate the end of a new sequence. Update $S_C(i,j)$ and $V(S_C(1, j-1))$ to $S_C(j+1, j+1)$(the single symbol in the $j+1$ position) and $V(S_C(1,j))$, respectively, and the step 2 continues.

3. This parsing operation begins with $S_C(1,1)$ and continues until $j = n$, where n is the length of the symbolic sequence S_C.

For instance, the sequence which is only composed of units 01 (i.e., $010101\cdots$) is parsed as $0 \cdot 1 \cdot 0101 \cdots$. So the number of distinct substrings $c(n)$ is 3. To compute the LZ complexity, the sequence of H and F should be transformed into a 0-1 symbolic sequence (i.e., map the H and F to 1 and 0). Follow the above method, the twelve randomly selected sequences in Fig.4 (from 1 to 12) are parsed as:

1. $1 \cdot 0 \cdot 101010101010101010\cdot \rightarrow c(n) = 3$
2. $1 \cdot 1110 \cdot 111101111011110\cdot \rightarrow c(n) = 3$
3. $1 \cdot 1111110 \cdot 0001 \cdot 111101 \cdot 11\cdot \rightarrow c(n) = 5$
4. $1 \cdot 0 \cdot 11 \cdot 010 \cdot 00 \cdot 111 \cdot 1001 \cdot 1010\cdot \rightarrow c(n) = 8$
5. $1 \cdot 110 \cdot 01 \cdot 101 \cdot 000 \cdot 111000 \cdot 11\cdot \rightarrow c(n) = 7$
6. $1 \cdot 0 \cdot 01 \cdot 110 \cdot 11100 \cdot 1010 \cdot 0110\cdot \rightarrow c(n) = 7$
7. $0 \cdot 01 \cdot 10 \cdot 0010 \cdot 0101 \cdot 1011011\cdot \rightarrow c(n) = 6$
8. $1 \cdot 10 \cdot 001 \cdot 111110 \cdot 010 \cdot 11101\cdot \rightarrow c(n) = 6$
9. $1 \cdot 11110 \cdot 01 \cdot 10010 \cdot 11101 \cdot 00\cdot \rightarrow c(n) = 6$
10. $1 \cdot 10 \cdot 001 \cdot 011 \cdot 0000 \cdot 1010 \cdot 101\cdot \rightarrow c(n) = 7$
11. $1 \cdot 10 \cdot 001 \cdot 1110 \cdot 0010 \cdot 0101 \cdot 11\cdot \rightarrow c(n) = 7$
12. $0 \cdot 01 \cdot 01011 \cdot 000 \cdot 001011 \cdot 111\cdot \rightarrow c(n) = 6$

3. DETAIL FORMS OF THE SEQUENCES IN FIG.5

1. $HFHFHFHFHFHFHFHFHFHF$
2. $HHHHFHHHHFHHHHFHHHHF$
3. $HHHHHHHFFFFHHHHHFHHH$
4. $HFHHFHFFFHHHHFFHHFHF$
5. $HHHFFHHFHFFFHHHFFFHH$
6. $HFFHHHFHHHFFHFHFFHHF$
7. $FFHHFFFHFFHFHHFHHFHH$
8. $HHFFFHHHHHHFFHFHHHFH$
9. $HHHHHFFHHFFHFHHHFHFF$
10. $HHFFFHFHHFFFFHFHFHFH$
11. $HHFFFHHHHFFFHFFHFHHH$
12. $FFHFHFHHFFFFFHFHHHHH$

REFERENCES

1. J. Hu, J. Gao, and J. C. Principe, "Analysis of biomedical signals by the lempel-ziv complexity: the effect of finite data size," IEEE Trans. Biomed. Eng. **53**, 2606–2609 (2006).